



Published in final edited form as:

Cell. 2015 April 9; 161(2): 277–290. doi:10.1016/j.cell.2015.02.016.

Organ-level quorum sensing directs regeneration in hair stem cell populations

Chih-Chiang Chen^{1,2,3}, Lei Wang⁴, Maksim V. Plikus⁵, Ting Xin Jiang¹, Philip J. Murray⁶, Raul Ramos⁵, Christian F. Guerrero-Juarez⁵, Michael W Hughes⁷, Oscar K. Lee⁸, Songtao Shi⁹, Randall B. Widelitz¹, Arthur D. Lander¹⁰, and Cheng Ming Chuong^{1,3,11,*}

¹Department of Pathology, University of Southern California, Los Angeles, California 90033, USA

²Department of Dermatology, Taipei Veterans General Hospital, Taipei, Taiwan

³Institute of Clinical Medicine and Department of Dermatology, National Yang-Ming University, Taipei, Taiwan

⁴State Key Laboratory of Military Stomatology, Department of Oral and Maxillofacial Surgery, School of Stomatology, The Fourth Military Medical University, Xi'an, Shaanxi 710032, China

⁵Department of Developmental and Cell Biology, Sue and Bill Gross Stem Cell Research Center, Center for Complex Biological Systems, University of California, Irvine, CA 92697, USA

⁶Division of Mathematics, University of Dundee, Scotland, DD1 4HN, UK

⁷International Laboratory of Wound Repair and Regeneration, National Cheng Kung University, Tainan, Taiwan

⁸Department of Orthopaedics and Traumatology, Taipei Veterans General Hospital, Taipei and Center for Stem Cell Research, National Yang-Ming University and Veterans General Hospital, Taipei, Taiwan

⁹Department of Anatomy and Cell Biology, University of Pennsylvania, School of Dental Medicine, Philadelphia, PA, USA

¹⁰Department of Developmental and Cell Biology, Department of Biomedical Engineering and Center for Complex Biological Systems, UC Irvine, Irvine, CA 92697, USA

¹¹Research Center for Developmental Biology and Regenerative Medicine, National Taiwan University, Taipei, Taiwan

© 2015 Published by Elsevier Inc.

*Corresponding author: Cheng-Ming Chuong, MD, PhD, Department of Pathology, Keck School of Medicine, University of Southern California, Los Angeles, California 90033, USA, Tel: 323-442-1296, Fax: 323-442-3049, cmchuong@usc.edu.

Publisher's Disclaimer: This is a PDF file of an unedited manuscript that has been accepted for publication. As a service to our customers we are providing this early version of the manuscript. The manuscript will undergo copyediting, typesetting, and review of the resulting proof before it is published in its final citable form. Please note that during the production process errors may be discovered which could affect the content, and all legal disclaimers that apply to the journal pertain.

AUTHOR CONTRIBUTIONS

CCC and CMC conceived the overall experimental design. CCC and TXJ did the hair plucking and characterization. LW, SS, MWH did immune characterization. ADL and PJM did mathematical modeling. ADL did mathematical estimation of length scale for quorum sensing. MVP, RR, CFG-J did LysM-Cre mouse work. CCC, CMC, ADL, MVP, RBW and OL did manuscript writing and editing.

SUMMARY

Coordinated organ behavior is crucial for an effective response to environmental stimuli. By studying regeneration of hair follicles in response to patterned hair removal, we demonstrate that organ-level quorum sensing allows coordinated responses to skin injury. Removing hair at different densities leads to a regeneration of up to 5 times more neighboring, unplucked resting hairs, indicating activation of a collective decision-making process. Through data modeling, the range of the quorum signal was estimated to be on the order of 1 mm, greater than expected for a diffusible molecular cue. Molecular and genetic analysis uncovered a two-step mechanism, where release of CCL2 from injured hairs leads to recruitment of TNF- α secreting macrophages, which accumulate and signal to both plucked and unplucked follicles. By coupling immune response with regeneration, this mechanism allows skin to respond predictively to distress, disregarding mild injury, while meeting stronger injury with full-scale cooperative activation of stem cells.

INTRODUCTION

The effective coordination of organ behavior, either under physiological conditions or as a response to injury, is essential for survival. Integration at the level of large-scale organ systems has been extensively studied, but the role of shorter range, local coordination has not. For example, is the regeneration of repeated tissue units within an organ (e.g. hair follicles (HFs) in skin, villi in intestine) coordinated so as to achieve collective decision-making? If so, what are the mechanisms of communication, and how is information integrated? In particular, if injury or malfunction affects only a subset of tissue units in an organ, how is such a collective decision made whether to mount a response that is local (e.g. local repair) or global (e.g. tissue level regeneration)?

Mammalian skin offers an excellent platform to address such questions, because its numerous HFs behave as discrete, repeating, semi-autonomous tissue units (Jahoda and Christiano, 2011) distributed on a two dimensional plane. HFs undergo cyclic regeneration (Paus et al., 1998) by regulating both intra- and extra-follicular cues for hair stem cell activation (Stenn and Paus, 2001; Plikus et al, 2008, 2011; Festa et al., 2011; Chen and Chuong, 2012), both during physiological regeneration and in response to injury (Chuong et al., 2012). The experimental accessibility of HFs makes them an ideal model to study collective decision making in an organ population *in vivo*.

Classical studies show that hair plucking produces a micro-injury that can potentially lead to hair regeneration (Collins, 1918; Silver and Chase, 1970). This process is thought to be mediated by an autonomous mechanism in each follicle, in which early apoptosis in the bulge leads to activation of hair germ progenitors (Ito et al, 2002). Here, we uncover evidence that the decision of hair stem cells to be activated or remain quiescent also depends on information coming from neighboring follicles. This possibility was first suggested by our earlier study in which plucking fewer than 50 refractory telogen hairs did not induce hair regeneration, while plucking more than 200 hairs did (Plikus et al., 2008). Here, by varying the spacing, arrangement and shapes of plucked regions, we unexpectedly found that plucking 200 hairs, with a proper topological distribution can cause up to 1200 hairs to

regenerate. These results demonstrate marked non-autonomy in HF regeneration, and a distinctly non-linear quantitative relationship between plucking and regeneration.

As discussed below, the collective HF response to injury may be seen as an example of quorum sensing, a form of social behavior in which population decisions depend on the density of signaling individuals within a given spatial territory (Bassler 2002; Pratt 2005). In order to gain insights into the possible mechanisms underlying this behavior, we first used mathematical modeling to identify the characteristic spatial range over which quorums are sensed, which led us to suspect that the signaling mechanism consists of more than just a diffusible molecule. The time course of molecular changes after plucking, together with the results of genetic and pharmacological manipulation, implicated a two-stage mechanism, involving the release of diffusible signals that recruit immune cells (M1 macrophages) which then actively spread among follicles, where they locally induce regeneration through the release of substances such as Tnf- α .

This work identifies a mechanism for quorum sensing that operates on the millimeter scale to coordinate the behaviors of semi-autonomous tissue units within an organ. Such coordination enables the skin to condition its responses to the spatial extent of injuries, launching a full scale regenerative response only when a sufficient threshold is reached.

RESULTS

Topology-dependent hair plucking can induce the regeneration of more hairs than were plucked by activating neighboring, unplucked follicles

To gain insight into the mechanisms leading to hair renewal following follicle injury, the relationship between hair plucking density and regeneration were examined in the mouse. To standardize the experiments, we synchronized all the dorsal pelage HFs into refractory telogen before plucking (see supplementary method). Normal hair density in adult C57BL/6 mouse dorsal skin is about 45–60 hairs/mm², corresponding to a distance between each follicle of around 0.15mm (Fig. S1E). In the first set of experiments, 200 evenly distributed refractory telogen hairs were plucked within a circular skin area (the “injury field”; Fig. 1B–C, red circle). By plucking a constant number of hairs but altering the size of the injury field (Fig. 1A, B, S1), plucking densities from 2–50 hairs/mm² were obtained (supplementary method, Fig. 1, S1). We then studied the regenerative behavior of the HFs.

We observe three types of responses (Fig. 1F). 1) If 200 hairs were plucked in a large area (> 6mm diameter, 28.3 mm², plucking density < 10 hairs/mm²; Fig. 1B, S1), no regeneration of plucked or unplucked follicles occurs even after 30 days (Fig. 1A, B, S1). This is because the plucking density is too low and doesn't generate accumulated signals above the threshold level (Fig. 1F, Zone of very low density plucking, gray area). 2) When 200 hairs are plucked from 3, 4, or 5 mm diameter circular areas (plucking density > 10 hairs/mm², the threshold density), we induce a simultaneous regeneration of the whole region (including the plucked and surrounding unplucked follicles; Fig. 1C–D). Thus, by plucking only 200 hairs, the eventual regeneration of approximately 450, 780 or 1300 hairs are obtained (with 200 hairs plucked in injury field sizes of 3, 4, 5 mm in diameter, or 7.1, 12.6 and 19.6 mm² respectively; Fig. 1C–F, S1–2). As an example, we can induce

regeneration of up to 600 unplucked hairs within a 5mm plucked region (Zone of quorum sensing-dependent hair regeneration, orange / light green area in Fig. 1F) and 400 hairs outside of the plucked region, resulting from propagation. 3) When 200 hairs are plucked from a 2.4 mm diameter region (high density, 100% plucking), every follicle in the field is plucked. (Fig. 1A). In this case, all follicles re-entered anagen about 12 days (12.3 ± 3.37 , $n=13$) after plucking and the number of regenerating follicles equals the number of plucked follicles (Zone of all follicles plucked, dark green). Plucking-dependent regeneration from refractory telogen requires the plucking of at least 50 follicles to reach the basal threshold (Plikus et al., 2008). This zone is equivalent to the frequently used wax stripping procedure (Muller-Rover et al., 2001) in which melted wax was used to strip away all follicles in a large region, usually centimeters in diameter or bigger. This method involves thousands of HFs which will regenerate in synchrony without using quorum sensing.

The hair follicle population as a quorum sensing system

The density-dependence of regeneration, together with the simultaneous regeneration of both plucked and unplucked follicles within the injury field, suggests that plucked follicles produce a signal that (a) spreads to neighboring follicles, (b) accumulates to a level that depends upon the density and position of other plucked follicles, and (c) when present above some threshold level will trigger any follicle—plucked or unplucked—to re-enter anagen.

The idea that HFs produce signals that affect other HFs can be inferred from the coordinated waves of hair cycling that travel across the skin of mice and rabbits (Plikus et al, 2008, 2011). Yet the signals that coordinate such “hair waves” cannot explain the collective regenerative responses seen here, at least not those within the injury field itself. This is because hair waves reflect the ability of follicles in anagen to accelerate the progression of neighboring telogen follicles into anagen, whereas plucking causes injured and uninjured follicles to progress from refractory telogen to regenerate collectively and simultaneously (i.e. regeneration is not driven by neighboring anagen follicles). Just outside the plucked injury fields (e.g. Fig. 1C, outside of the red circle), however, the ring of delayed regeneration likely reflects the “hair wave” phenomenon, since follicles in this zone enter anagen only after regeneration in neighboring follicles is well underway. To avoid confusion between initial, collective regeneration and later hair wave spreading, the present study focuses exclusively on early regenerative events.

One way to gain insight into the nature of the quorum signal—which we shall initially call the “distressor”—that coordinates collective regeneration is to characterize its decay length, i.e. the characteristic spatial scale over which the strength of the signal decays. Decay lengths quantify the balance between the rate at which a signal spreads and the rate at which it is destroyed or removed. Diffusible molecules that are captured by high-affinity, cell surface receptors— e.g., morphogens, growth factors, cytokines and chemokines— tend to have relatively short decay lengths, typically on the order of no more than 100 μm (e.g. Teleman and Cohen, 2000; Müller et al., 2012; Sarris et al., 2012; Weber et al., 2013; Shimozone et al., 2013), roughly the same scale as the inter-follicular distance in mouse skin. In contrast, as we show in the next section, the decay length of the putative distressor

induced by plucking appears to be substantially larger—on the order of 1 mm, or 4–6 inter-follicular distances.

Estimating the range of action of the quorum signal

Regardless of the physical nature of a signal (i.e., if it spreads from cell to cell via an undirected random walk), its spread can usually be modeled as a diffusion process, and it will display a decay length, λ , equal to the square root of the ratio between its diffusivity (an intrinsic measure of how fast it moves) and the rate constant that characterizes its removal or destruction in the tissue through which it spreads (Lander 2007; a physical interpretation of λ is the distance over which the steady-state signal from a point source falls by a factor of $1-1/e$, or about 63%).

The results of modeling plucked hairs as an array of point sources of a diffusible distressor in a two-dimensional medium (Fig. 2A, also see Supplement methods) tell us that the expected steady-state distressor concentration should be a function not only of plucking density, but also of injury field size, shape, and λ . For example, with a constant plucking density, concentrations of distressor should rise as a function of field size/ λ , leveling off as that ratio gets large (Fig. 2A). Assuming that regeneration is triggered when the distressor concentration around a HF exceeds a certain threshold, these results suggest that one could estimate the value of λ from a series of experiments in which plucking density and injury size/shape are both varied.

For example, in Fig. 2B, data on whether regeneration in circular injury fields occurred (green dots) or failed (red dots) was tabulated as a function of field radius and plucking density (plotted, in this case, as the inverse of the plucked fraction). Fitting the boundary between positive and negative data to the predictions of the steady state diffusion model yields estimates of λ between 0.6 and 1.6 mm (Supplementary method).

The same model also predicts that, for sufficiently large plucked fields and/or sufficiently high plucking densities, immediate regenerative responses should not be limited to the precise boundaries of the injury field, but should extend a small distance beyond those boundaries (here we refer only to regeneration that occurs at the same time as that within the injury field, and not what is triggered significantly later by hair wave propagation). Careful examination of experimental data showed that a small rim of early regeneration indeed occurred just outside of some injury fields. Fitting the sizes of these rims to the model (Fig. 2C) yields an independent estimate for $\lambda = 1$ mm.

Finally, the same diffusion model suggests that λ can also be estimated by holding both plucking density and injury field area constant, but varying the shape of the injury field. To test this prediction, experiments were carried out in which 50 hairs were plucked evenly at a density of every other hair, either in a straight line (Fig. 2D), a narrow rectangle (6:1 aspect ratio; Fig. 2E) or a square (Fig. 2F). Under these distinct topological conditions, plucked single rows never regenerated, while squares always regenerated robustly. Rectangles occasionally exhibited modest regeneration, suggesting a distressor concentration very close to threshold under these circumstances. Fitting these three behaviors requires a value of λ between 0.7 and 1.2 mm.

The good agreement among these three methods supports the validity of the steady state diffusion model for describing distressor spreading, and places the value of λ at approximately 1 mm. Fitting to the model does not imply, however, that the distressor is a single substance, or even a diffusible molecule, but simply that it spreads according to the same rules. In fact, the observed magnitude of λ suggests that the distressor is not simply a diffusible receptor-binding molecule, since these typically display decay lengths of one tenth this magnitude or less (e.g. Teleman and Cohen, 2000; Müller et al., 2012; Sarris et al., 2012; Weber et al., 2013; Shimozono et al., 2013). As described below, further investigation of the molecular nature of the distressor signal supports the idea that it consists of both diffusible molecules and recruited cells that migrate actively between follicles.

Plucking induces a cascade of inflammatory, cellular and molecular events

Results from wax-stripping experiments indicate that HF keratinocytes undergo apoptosis around 4 hours after injury (Ito et al, 2002; see also Fig. 3A). To identify molecules and mechanisms that might be involved in plucking-induced regeneration, we carried out microarray analysis of plucked fields at 12, 24, 48, and 96 hours after injury. Among the notable, time-dependent changes in gene expression, we observed:

1) Transient increase in expression of pro-inflammatory cytokines—Immune, inflammatory and wound healing response genes constitute the major portion of early transcriptional activity following plucking. Analyzing the most altered genes by RT-PCR, we found that immune cytokines, *chemokine (C-C motif) ligand 2 (CCL2)*, *chemokine (C-X-C motif) ligand 2 (CXCL2)*, and *interleukin 1, beta (IL-1 β)* were up-regulated soon after plucking (i.e., 12hrs), although expression of these genes peaked at different times (Fig. 3B). For example, *CCL2* expression peaked around 12hrs (Fig. 3B).

2) Reduced refractory telogen inhibitor expression—During refractory telogen, the extra-follicular macro-environment expresses high levels of inhibitors, including *Bmp2*, *Dickkopf (Dkk1)* and *soluble frizzled related protein (Sfrp4)* that block anagen re-entry and hair wave propagation (Plikus et al, 2008, 2011). Expression of *Sfrp4*, a representative gene, decreased markedly at day 1 but rebounded by day 2 and 4 (Fig. 3B).

3) Increased tumor necrosis factor alpha (Tnf- α) expression—*Tnf- α* increases between 1–2 days after plucking and reached a plateau at about day 2 (Fig. 3B, C). The plateau of *Tnf- α* expression corresponds to a time when activated hairs are in early anagen phase (Fig. 3C). We also observe changes of other molecular pathways. For example, *platelet derived growth factor A (Pdgf- α)* increased at later stages after plucking (day 4), compatible with published results (Festa et al, 2011) (Fig. 3B).

Since the Wnt pathway is critical for hair growth (Enshell-Seijffers et al, 2010; Lowry et al, 2005), we examined the expression of Wnt pathway members, using whole mount in situ hybridization, and compared their expression patterns, over time, with those of *Tnf- α* . *Wnt6*, *β -catenin*, and *lymphocyte enhancer factor (Lef-1)* were up-regulated within new anagen follicles at day 4, but not in the extra-follicular dermal macro-environment (Fig. S3). We

also localized *Tnf- α* expression to the extra-follicular dermal macro-environment (Fig. 3C, S3).

CCL2 is a key component of the quorum signal

The earliest noted signaling molecule expression change that could potentially communicate information from plucked to unplucked follicles was CCL2 (Fig. 3B).

Immunohistochemistry showed that CCL2 is primarily produced by HF keratinocytes, and accumulates predominantly in plucked follicles (where apoptosis occurs), and to a much smaller extent in neighboring unplucked follicles, which do not undergo apoptosis (Fig. 4A, 4B, S4). This induction is transient and diminishes at day 5. CCL2 induction in plucked HFs occurred regardless of plucking density, so CCL2 was expressed even at the densities that failed to launch regeneration. Epidermal staining of CCL2 is evident in the 2.4 mm specimen, some is seen surrounding the plucked follicle in the 5 mm specimen, but staining is sparse in the 8 mm specimen.

These results are consistent with CCL2 expression providing an overall measure of the extent of plucking, and therefore potentially serving as a quorum signal. To test whether CCL2 function is required for follicle regeneration, we waxed whole back skin from both wild type C57BL/6 and CCL2 null mice. In contrast to the localized plucking of 200 hairs (which induces hair regeneration after about 12 days (Plikus et al., 2008)), wax-stripping the whole back skin drives telogen hairs back into full anagen (anagen VI) within about 6 days (Muller-Rover *et al.*, 2001). However, when the backs of CCL2 null mice were wax-stripped, follicles remained in telogen 3 days after waxing, and were still in anagen III to IV at day 6 (Fig. 4C, S5A). This delayed hair regrowth in CCL2 null mice following plucking supports a role for CCL2 in plucking induced hair regeneration.

TUNEL staining performed 1 day after plucking revealed that both wild type and CCL2 null mice showed apoptotic HF cells (Fig. 4D, S5B). These results indicate that CCL2 is not required for the initial injury response of HFs, but rather its expression is triggered by that response, whereupon it plays an important role in regeneration. This view is consistent with a recent study showing that various HF regions express chemokines including CCL2, CCL20 and CCL8 in response to stress (Nagao et al, 2012a). The percent HF area with CCL2 expression was highest 1 day after plucking and decreased thereafter (Fig. 4E). Unplucked follicles located within (x) or outside (y) of the plucked field showed low and no CCL2 levels. CCL2 null mice did not express CCL2 after plucking (z).

M1 macrophages are mediators recruited by CCL2 to execute quorum sensing behavior

The decay lengths of most diffusible signaling molecules, including chemokines (Sarris et al., 2012; Weber et al., 2013), are much shorter than the decay length we measured for the plucking-induced quorum signal (Fig. 2). Chemokines, however, are known to act as chemo-attractants for immune cells, and we postulated that this might play a role in boosting the effective range of action of an initial quorum signal. CCL2 in particular is a potent recruiter of monocyte/macrophage lineage cells.

Indeed, two days after plucking, macrophages had heavily infiltrated the plucked skin (Fig. 5A). We quantified the macrophage distribution at different times after plucking (Fig. 5E). At day 1, F4/80 positive macrophages accumulate around and between the plucked follicles. At day 3, more macrophages spread to the inter-plucked follicular regions and their density is substantially elevated (at least four times over background) up to 66 % of that found for plucked follicles. The spread can span a distance of 1mm. These macrophages start to dissipate at day 7 post-plucking.

To test whether macrophages play a functional role in plucking-induced hair regeneration we used chemical inhibitor and genetic deletion assays. The application of Clodronate liposomes to suppress macrophage function caused an approximately 12 day delay in hair plucking induced regeneration (Fig. 6F). For the genetic approach, we used *LysM-Cre;R26R* transgenic mice to examine the distribution of LacZ positive myeloid cells following hair plucking. Myeloid cells are nearly absent in normal mice, but are induced at day 3–5, and diminish at day 7 in the transgenic mice (Fig. 5F).

To evaluate their role, we generated a triple transgenic mouse model where myeloid cells are specifically depleted by diphtheria toxin upon doxycycline treatment (*LysM-Cre;Rosa-rtTA;TetO-DTA*). We plucked 200 hairs / 5 mm diameter region, which usually launches a quorum sensing response, leading to regeneration. In this mutant, hair regeneration did not occur (Fig. 5G, S2D). These myeloid cells represent mainly macrophages, although technically we cannot rule out other cell types completely. All together, the data suggest macrophages play a major role in this process.

Macrophages can be divided into two major types; M1 macrophages (classically activated) exert proinflammatory activities; while M2 macrophages (alternatively activated) are involved in resolving inflammation (Gordon, 2003; Willenborg et al, 2012). Immunostaining showed that M1, but not M2 macrophages, were present 5 days post-plucking (Fig. 5B–C, S6A).

These findings are consistent with other studies implicating chemokines in the recruitment of inflammatory macrophages during wound healing and a role for such cells in tissue repair (Willenborg et al, 2012). Since M1 macrophages express CCR4 (Fig. 5D, S6A), the receptor for CCL2, we think that these macrophages are recruited to plucked follicles by plucking-induced CCL2. Consistent with this view, plucking failed to induce the accumulation of M1 macrophages in CCL2 null mouse skin (Fig. 5H). These data support the model that CCL2 expressed by plucked follicles recruits CCR4-expressing M1 macrophages, which play an essential role in regeneration. We next explored how this comes about.

Hair regeneration induced by quorum sensing is Tnf- α dependent

Macrophages are known to produce Tnf- α . *Tnf- α* mRNA was induced about 2 days after plucking, before anagen initiates (Fig. 3B–C, S3). Low power whole mount in situ hybridization reveals that, under conditions in which regeneration occurs, Tnf- α is enriched in the extra-follicular environment of both plucked and unplucked hairs (Fig. 6A). Double immunostaining showed that these cells are indeed M1 macrophages (Fig. 5B–D, 6B, S6).

Semi-quantitative analysis of immunostained specimens obtained from regions of different plucking densities support the view that Tnf- α expressing macrophages accumulate around HFs that regenerate after plucking (both plucked and unplucked), but do not accumulate under plucking conditions that fail to activate hair regeneration (Fig. S6D).

Quantitative measurements of macrophage derived Tnf- α immunoreactivity over time in a threshold plucking density region (200 hairs/5mm diameter) showed that Tnf- α positive cells are induced around plucked follicles. They then increased significantly at day 3 and 5 after plucking, spreading into the dermal region between plucked follicles. They decreased at day 7 to approach basal levels (Fig. 5E, 6C, S7B).

To investigate the functional importance of Tnf- α in plucking-induced hair regeneration, beads coated with Tnf- α related peptide were injected into refractory telogen stage mouse skin. Hair regeneration was induced, followed by propagation to the surrounding region (Fig. 6E). Control bead injection didn't induce hair regeneration even after 30 days (Fig. 6G). Conversely, when hairs were plucked at high density in Tnf- α null mice (Fig. 6F), a 15 day delay in regeneration was observed. These results indicate that Tnf- α is one of the major players for plucking-induced hair regeneration.

Lastly, we searched for molecules and signals that might function further downstream in hair regeneration. For example, Tnf- α is known to stimulate both JNK and NF- κ B (Nuclear factor kappa-light-chain-enhancer of activated B cell) signaling. It is also known that activation of the FGF signaling pathway can trigger hair regeneration (Greco et al., 2009). We therefore screened inhibitors of NF- κ B, JNK, PI3K, FGF receptor, p38 MAPK, and Erk for effects on plucking-induced hair regeneration. Only NF- κ B inhibitors delayed hair regeneration, doing so by 10 days (Fig. 6H, S7C). In addition, Tnf- α related peptide significantly stimulates the expression of Wnt3, Wnt10a and Wnt10b in keratinocytes (Fig. 6I). Though the Eda- NF- κ B pathway is important in hair development, a previous study indicated that Eda participates in anagen to catagen transition during the postnatal hair regeneration cycle (Fessing MY et al., 2006). Hence it is not likely that Eda is involved in the plucking induced hair regeneration response. Together the results raise the possibility that Tnf- α , acting through the NF- κ B pathway, ultimately stimulates hair regeneration through activation of Wnt signaling.

DISCUSSION

Social behaviors in an organ population

Many organs are composed of repeated, semi-autonomous tissue units, such as acini, crypts, and follicles. The potential for dynamic coupling between the behaviors of such units creates opportunities for collective phenomena. A dramatic example of this is the "hair wave", a coordinated hair cycle wave that can travel across the skin of mammals (Suzuki et al., 2003; Plikus et al., 2008, 2011; Murray et al., 2012).

In this work, we characterize another collective behavior of HFs; density- and topology-dependent, plucking-induced regeneration, which can be viewed as a form of quorum sensing. Quorum sensing is a process whereby a population makes a collective decision

based on the number or density of individuals that meet a certain criterion. Typically, a response occurs only when a threshold is exceeded. Quorum sensing has been invoked to describe bacterial cell-to-cell communication (Bassler 2002) that serves to influence gene regulation in response to population density fluctuations (Miller and Bassler, 2001). Synthetic quorum sensing circuits in yeast were used to demonstrate the diversity of social behaviors that can come from collective communication (Youk and Lim 2014). Quorum sensing also has been used to explain the collective decision-making behavior of social insects such as ants and honey bees (Pratt 2005; Visscher 2007).

Molecular nature of the quorum sensing circuit

Briefly, the quorum sensing circuit we describe here provides a way for injured HFs to collectively assess the magnitude and extent of injury that the skin has sustained, and make an all-or-none decision whether or not to regenerate. A striking feature of this circuit, revealed through molecular modeling, is that the information being shared among follicles decays with a characteristic length of about 1 mm, substantially greater than the measured decay lengths of diffusible signaling molecules (e.g. Teleman and Cohen, 2000; Müller et al., 2012; Sarris et al., 2012; Weber et al., 2013; Shimozone et al., 2013). The explanation for this apparent paradox seems to reside in the multi-stage nature of the quorum signal, which begins with diffusible molecules, but eventually involves the recruitment of motile cells (inflammatory macrophages) that spread within the tissue. Below we summarize the sequence of molecular and cellular events revealed by the present study (Fig. 7).

(i) Micro-injury and inflammation—Hair plucking leads to hair keratinocyte apoptosis (Ito et al, 2002; Fig. 3A). This in turn leads to inflammatory changes, and to the localized over-expression of several inflammatory cytokines, especially CCL2, which may be detected within 12 hours post-plucking (Fig. 3B, 4).

(ii) Molecular signal release and dissemination—CCL2 and other cytokines are secreted from plucked follicles and may also involve epidermis around the plucked follicle. The importance of CCL2 is demonstrated by the fact that, in CCL2-null skin, regeneration is markedly delayed (Fig. 4). The fact that it is not prevented entirely suggests that some other cytokines induced by plucking may act redundantly with CCL2.

(iii) Recruitment of macrophages as motile vectors—The local production of CCL2 appears to recruit CCR4 (+) M1 macrophages in the dermis (Fig. 5). Whereas macrophages initially appear to be enriched around plucked follicles, recruited macrophages soon spread throughout the whole region. By relaying a signaling response with a motile cellular vector, HFs effectively solve the problem of spreading quorum information over long distances.

Another motile vector candidate is the epidermal dendritic Langerhans cell since it also expresses F4/80 antigen. However, F4/80 positive cells appear in dermis at day 1, but do not appear in the epidermis until day 5–7. Our microarray data also did not reveal up-regulation of Langerhans cell markers, such as CD207 (Langerin) and CD11b. Although we do not completely rule out the involvement of Langerhans in this process, our data so far suggest a major role for dermal macrophages in this process.

It is worthwhile to mention here that more examples of extended cellular process that mediate signal communication are being identified. For example, in zebrafish stripe pattern formation, pigment cells can utilize their contact-dependent depolarization and repulsive behavior as non-diffusible inhibitors that follow Turing principles (Inaba et al., 2012). In *Drosophila epithelia*, cytonemes can establish a dynamic hedgehog morphogen gradient that may reach afar (Bischoff et al., 2013). Future *in vivo* imaging studies of the mouse skin model studied here will allow us to elucidate the interactive cellular behaviors between HFs, immune system and regeneration.

iv) Release of Tnf- α and collective regeneration—Inflammatory macrophages that are recruited to wound fields secrete Tnf- α , which has been shown to activate hair cycle regeneration (Fig. 6E; Duheron et al, 2011). Regeneration is greatly impaired in Tnf- α -null mice (Fig. 6F); moreover, Tnf- α serum levels are normal in CCL2-null mice that show impaired plucking-induced regeneration (Fig. 5I). These studies indicate that local, not systemic Tnf- α is required for regeneration. Although the exact mechanism by which Tnf- α triggers follicle regeneration is not clear, the data suggest that Tnf- α may act through NF- κ B which in turn activate canonical WNT signaling (Fig. 6D; Cawthorn et al, 2007; Schwitalla et al, 2013). While Tnf- α immunoreactivity is mainly in macrophages, it is also detected in other cell types and may provide additional possible mechanisms. The EDAR pathway may also activate NF- κ B. However, EDAR it is more involved in anagen/catagen transition (Fessing et al., 2006), not telogen/anagen transition. Further, it is not induced in our microarray data (not shown).

Adaptive role of quorum sensing

Depending on the severity of skin injury, the body may use different mechanisms to alert, defend and regenerate the damaged tissue. Plucking of a single hair follicle is a micro-injury. An open, full-thickness wound is a catastrophic event, i.e. macro-injury. While wounded skin is known to induce hair regeneration, small and large wounds may share a fundamental mechanism, but use different molecular circuits to achieve different levels of restoration and regeneration. Indeed, HF activities have been linked to the wound-healing and regenerative behaviors of the inter-follicular epidermis. This link may be mediated by the immune system (Paus et al, 1998), macrophage recruitment (Osaka et al, 2007) and increased Tnf- α expression (Jiang et al, 2010). Interestingly, TNF- α converting enzyme, a regulator of Tnf- α , is a component of the HF bulge niche (Nagao et al, 2012b). Anagen phase HFs can influence the surrounding epidermis to markedly accelerate wound healing (Ansell et al., 2011). In mice, loss of full thickness skin larger than 1 cm in diameter could lead to new follicle formation (Ito et al., 2007). However, plucking does not launch a full wound healing response, so conceptually plucking works differently from the wound and our study focuses at a different scale. It provides a novel understanding into how HFs respond to injury at the level of a HF population. We analyzed how interactions among HFs and the dermal environment reach a binary choice based on a collective measurement of injury. We show that effective damage control is achieved via co-option of existing signaling mechanisms (e.g., Tnf- α , macrophage) for the “social behaviors” of a stem cell population.

In summary, we report a higher level integration of signals from hair regeneration, immune cytokines and wound healing. Instead of a top-down process, quorum sensing represents a bottom-up process based on local information. Each follicle becomes a sensor for the population to assess the level of damage. The molecular circuit quantifies injury strength by summing together local signals from different organs. Here the communication among tissues reaches a larger scale organization by coupling local molecular signaling (in the form of a chemical gradient) with motile cellular vectors. In this study, macrophages are identified as a motile vector that allows a length scale of up to 1 mm. In this manner, the injury response is measured and reflects local needs. This study may just be one of the examples that reveal collective cellular behaviors in response to physiological or pathological stimuli. We believe that the quorum sensing behavior principle is likely to be present in the regeneration of tissue and organs beyond the skin.

EXPERIMENTAL PROCEDURES

Surgical procedures

All procedures were performed on anaesthetized animals with protocols approved by the USC IACUC. Hair cycle was synchronized by wax stripping (Muller-Rover *et al.*, 2001). Hairs in refractory telogen were plucked with the spacing indicated in the result section. Regenerative hair numbers are counted under a dissection microscope.

RNA preparation and microarray

For microarray, all cells in the region were used without micro-dissection or sorting. RNA was prepared using TRI Reagent BD (Sigma-Aldrich, Inc.) following the manufacturer's recommendations. Please see supplement methods for detail. The microarray data reported here have been submitted to the GEO (accession number GSE46181). Primer sequences for RT-PCR are listed in supplementary table 1.

Perturbation of quantitative plucking

Small molecular inhibitor or peptides were injected intra-dermally on one side of mouse dorsal skin for 4 days. Then 200 hairs were plucked in the center of the injected area. After plucking, these drugs were continuously injected for an additional 6 days. DMEM was injected to the opposite side as a control. Each animal was injected with only one reagent.

Supplementary Material

Refer to Web version on PubMed Central for supplementary material.

ACKNOWLEDGEMENTS

CMC, TXJ, RBW are supported by NIAMS R01-AR42177, AR 47364 and AR60306. CCC is supported by NSC 100-2314-B-075-044, NSC 101-2314-B-075-008 -MY3, Taipei Veterans General Hospital (VN103-12, V103C-010, V102B-009, R-1100403). ST Shi and Lei Wang are supported by NIH R01DE17449. MVP is supported by NIAMS R01-AR067273 and Edward Mallinckrodt Jr. Foundation grant. RR by CIRM training grant (TG2-01152), CFGJ is supported by the National Science Foundation Graduate Research Fellowship Program. (DGE-1321846). MWH is supported by Top Notch University plan of CKU, Taiwan. We thank Drs. Jaw-Ching Wu, Han-Nan Liu, Yun-Ting Chang of National Yang Ming University / Taipei Veterans General hospital for their

support. Invention number 2014-255 "Enhance hair growth via plucking" (D2014-0054) was disclosed to University of Southern California.

REFERENCES

- Ansell DM, Kloeppe JE, Thomason HA, Paus R, Hardman MJ. Exploring the "hair growth-wound healing connection": anagen phase promotes wound re-epithelialization. *J. Invest. Dermatol.* 2011; 131:518–528. [PubMed: 20927125]
- Bassler BL. Small talk. Cell-to-cell communication in bacteria. *Cell.* 2002; 109:421–424. [PubMed: 12086599]
- Bischoff M, Gradilla AC, Seijo I, Andrés G, Rodríguez-Navas C, González-Méndez L, Guerrero I. Cytosomes are required for the establishment of a normal Hedgehog morphogen gradient in *Drosophila* epithelia. *Nat. Cell Biol.* 2013; 15:1269–1281. [PubMed: 24121526]
- Cawthorn WP, Heyd F, Hegyi K, Sethi JK. Tumour necrosis factor- α inhibits adipogenesis via a beta-catenin/TCF4(TCF7L2)-dependent pathway. *Cell Death. Differ.* 2007; 14:1361–1373. [PubMed: 17464333]
- Chen CC, Chuong CM. Multi-layered environmental regulation on the homeostasis of stem cells: the saga of hair growth and alopecia. *J. Dermatol. Sci.* 2012; 66:3–11. [PubMed: 22391240]
- Chuong CM, Randall VA, Widelitz RB, Wu P, Jiang TX. Physiological regeneration of skin appendages. *Physiology.* 2012; 27:61–72. [PubMed: 22505663]
- Collins HH. Studies of normal moult and of artificially induced regeneration of pelage in *Peromyscus*. *J. Exp. Zool.* 1918; 27:73–99.
- Duheron V, Hess E, Duval M, Decossas M, Castaneda B, Klöpffer JE, Amoasii L, Barbaroux JB, Williams IR, Yagita H, et al. Receptor activator of NF- κ B (RANK) stimulates the proliferation of epithelial cells of the epidermo-pilosebaceous unit. *Proc. Natl. Acad. Sci. U S A.* 2011; 108:5342–5347. [PubMed: 21402940]
- Enshell-Seijffers D, Lindon C, Kashiwagi M, Morgan BA. Activity in the Dermal Papilla Regulates Morphogenesis and Regeneration of Hair. *Dev. Cell.* 2010; 18:633–642. Beta-Catenin. [PubMed: 20412777]
- Fessing MY, Sharova TY, Sharov AA, Atoyan R, Botchkarev VA. Involvement of the Edar signaling in the control of hair follicle involution (catagen). *Am J Pathol.* 2006; 169:2075–2084. [PubMed: 17148670]
- Festa E, Fretz J, Berry R, Schmidt B, Rodeheffer M, Horowitz M, Horsley V. Adipocyte lineage cells contribute to the skin stem cell niche to drive hair cycling. *Cell.* 2011; 146:761–771. [PubMed: 21884937]
- Gordon S. Alternative activation of macrophages. *Nat. Rev. Immunol.* 2003; 3:23–35. [PubMed: 12511873]
- Greco V, Chen T, Rendl M, Schober M, Pasolli HA, Stokes N, Dela Cruz-Racelis J, Fuchs E. A two-step mechanism for stem cell activation during hair regeneration. *Cell Stem Cell.* 2009; 4:155–169. [PubMed: 19200804]
- Inaba M, Yamanaka H, Kondo S. Pigment pattern formation by contact-dependent depolarization. *Science.* 2012; 335:677. [PubMed: 22323812]
- Ito M, Kizawa K, Toyoda M, Morohashi M. Label-retaining cells in the bulge region are directed to cell death after plucking, followed by healing from the surviving hair germ. *J. Invest. Dermatol.* 2002; 119:1310–1316. [PubMed: 12485433]
- Ito M, Yang Z, Andl T, Cui C, Kim N, Millar SE, Cotsarelis G. Wnt-dependent de novo hair follicle regeneration in adult mouse skin after wounding. *Nature.* 2007; 447:316–320. [PubMed: 17507982]
- Jahoda CA, Christiano AM. Niche crosstalk: intercellular signals at the hair follicle. *Cell.* 2011; 146:678–681. [PubMed: 21884930]
- Jiang S, Zhao L, Teklemariam T, Hantash BM. Small cutaneous wounds induce telogen to anagen transition of murine hair follicle stem cells. *J. Dermatol. Sci.* 2010; 60:143–150. [PubMed: 21071180]

- Lander AD. Morpheus Unbound: Reimagining the Morphogen Gradient. *Cell*. 2007; 128:245–256. [PubMed: 17254964]
- Lowry WE, Blanpain C, Nowak JA, Guasch G, Lewis L, Fuchs E. Defining the impact of beta-catenin/Tcf transactivation on epithelial stem cells. *Genes. Dev.* 2005; 19:1596–1611. [PubMed: 15961525]
- Miller MB, Bassler BL. Quorum sensing in bacteria. *Annu. Rev. Microbiol.* 2001; 55:165–199. [PubMed: 11544353]
- Müller P, Rogers KW, Jordan BM, Lee JS, Robson D, Ramanathan S, Schier AF. Differential diffusivity of Nodal and Lefty underlies a reaction-diffusion patterning system. *Science*. 2012; 336:721–724. [PubMed: 22499809]
- Muller-Rover S, Handjiski B, van der Veen C, Eichmüller S, Foitzik K, McKay IA, Stenn KS, Paus R. A comprehensive guide for the accurate classification of murine hair follicles in distinct hair cycle stages. *J. Invest. Dermatol.* 2001; 117:3–15. [PubMed: 11442744]
- Murray PJ, Plikus MV, Maini PK, Chung CM, Baker RE. Modelling hair follicle growth dynamics as an excitable medium. *PLoS Comp. Bio.* 2012; 8:e1002804.
- Nagao K, Kobayashi T, Moro K, Ohyama M, Adachi T, Kitashima DY, Ueha S, Horiuchi K, Tanizaki H, Kabashima K, et al. Stress-induced production of chemokines by hair follicles regulates the trafficking of dendritic cells in skin. *Nat. Immunol.* 2012a; 13:744–752. [PubMed: 22729248]
- Nagao K, Kobayashi T, Ohyama M, Akiyama H, Horiuchi K, Amagai M. Brief Report: Requirement of TACE/ADAM17 for Hair Follicle Bulge Niche Establishment. *Stem Cells*. 2012b; 30:1781–1785. [PubMed: 22696231]
- Osaka N, Takahashi T, Murakami S, Matsuzawa A, Noguchi T, Fujiwara T, Aburatani H, Moriyama K, Takeda K, Ichijo H. ASK1-dependent recruitment and activation of macrophages induce hair growth in skin wounds. *J. Cell Biol.* 2007; 176:903–909. [PubMed: 17389227]
- Paus R, van der Veen C, Eichmüller S, Kopp T, Hagen E, Muller-Rover S, Hofmann U. Generation and cyclic remodeling of the hair follicle immune system in mice. *J. Invest. Dermatol.* 1998; 111:7–18. [PubMed: 9665380]
- Plikus MV, Mayer JA, de la Cruz D, Baker RE, Maini PK, Maxson R, Chuong CM. Cyclic dermal BMP signalling regulates stem cell activation during hair regeneration. *Nature*. 2008; 451:340–344. [PubMed: 18202659]
- Plikus MV, Baker RE, Chen CC, Fare C, de la Cruz D, Andl T, Maini PK, Millar SE, Widelitz R, Chuong CM. Self-organizing and stochastic behaviors during the regeneration of hair stem cells. *Science*. 2011; 332:586–589. [PubMed: 21527712]
- Pratt SC. Quorum sensing by encounter rates in the ant *Temnothorax albipennis*. *Behav. Ecol.* 2005; 16:488–496.
- Sarris M, Masson JB, Maurin D, Van der Aa LM, Boudinot P, Lortat-Jacob H, Herbomel P. Inflammatory chemokines direct and restrict leukocyte migration within live tissues as glycan-bound gradients. *Curr. Biol.* 2012; 22:2375–2382. [PubMed: 23219724]
- Schwitalla S, Fingerle AA, Cammareri P, Nebelsiek T, Göktuna SI, Ziegler PK, Canli O, Heijmans J, Huels DJ, Moreaux G, et al. Intestinal Tumorigenesis Initiated by Dedifferentiation and Acquisition of Stem-Cell-like Properties. *Cell*. 2013; 152:25–38. [PubMed: 23273993]
- Shimozono S, Iimura T, Kitaguchi T, Higashijima S, Miyawaki A. Visualization of an endogenous retinoic acid gradient across embryonic development. *Nature*. 2013; 496:363–366. [PubMed: 23563268]
- Silver AF, Chase HB. DNA synthesis in the adult hair germ during dormancy (telogen) and activation (early anagen). *Dev. Biol.* 1970; 21:440–451. [PubMed: 5436903]
- Stenn KS, Paus R. Controls of hair follicle cycling. *Physiol. Rev.* 2001; 81:449–494. [PubMed: 11152763]
- Suzuki N, Hirata M, Kondo S. Traveling stripes on the skin of a mutant mouse. *Proc. Natl. Acad. Sci. U S A.* 2003; 100:9680–9685. [PubMed: 12893877]
- Teleman AA, Cohen SM. Dpp gradient formation in the *Drosophila* wing imaginal disc. *Cell*. 2000; 103:971–980. [PubMed: 11136981]
- Visscher PK. Group decision making in nest-site selection among social insects. *Annu. Rev. Entomol.* 2007; 52:255–275. [PubMed: 16968203]

- Weber M, Hauschild R, Schwarz J, Moussion C, de Vries I, Legler DF, Luther SA, Bollenbach T, Sixt M. Interstitial dendritic cell guidance by haptotactic chemokine gradients. *Science*. 2013; 339:328–332. [PubMed: 23329049]
- Willenborg S, Lucas T, van Loo G, Knipper JA, Krieg T, Haase I, Brachvogel B, Hammerschmidt M, Nagy A, Ferrara N, et al. CCR2 recruits an inflammatory macrophage subpopulation critical for angiogenesis in tissue repair. *Blood*. 2012; 120:613–625. [PubMed: 22577176]
- Youk H, Lim WA. Secreting and Sensing the Same Molecule Allows Cells to Achieve Versatile Social Behaviors. *Science*. 2014; 343:1242782. [PubMed: 24503857]

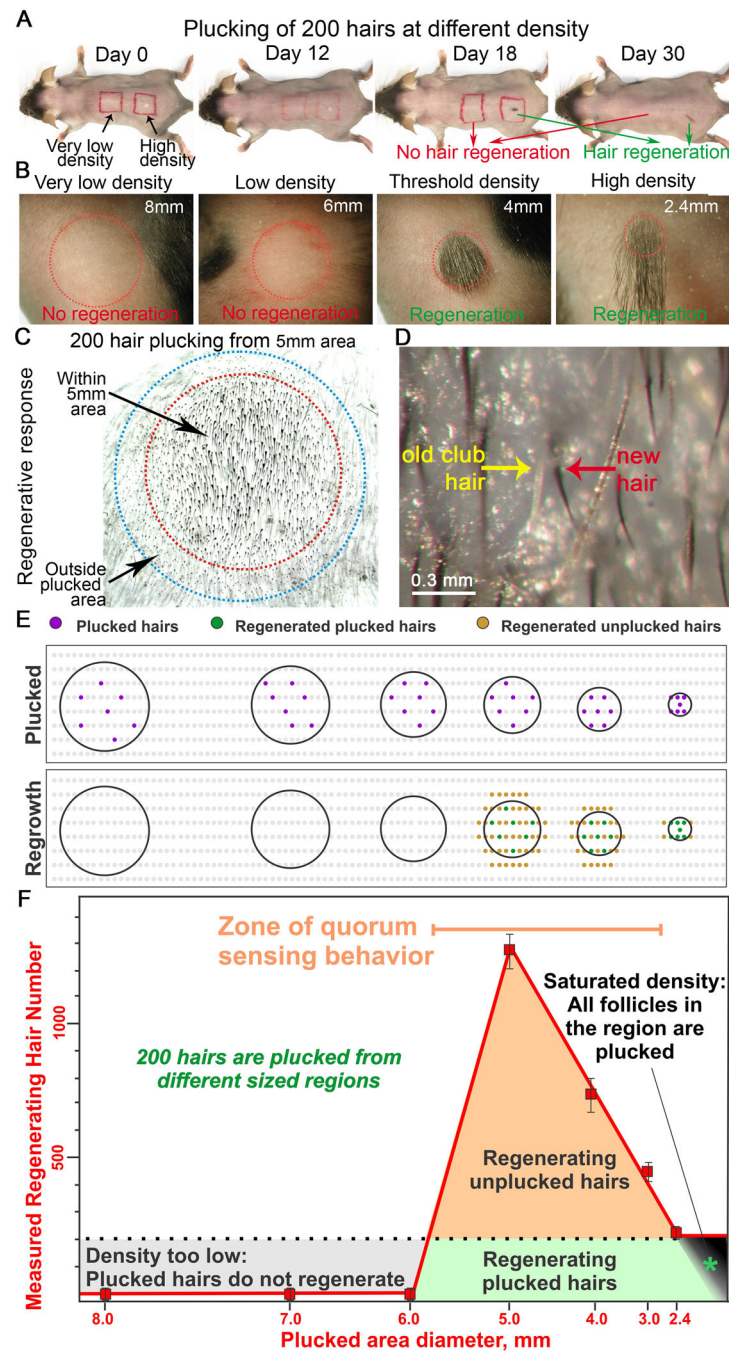


Figure 1. Plucking-induced hair regeneration is a population based behavior which depends on the density and distribution of plucked-hair follicles within the unplucked follicle population (A, B) Plucking 200 hairs from a circular 2.4 mm in diameter area (100% plucking) leads to hair regeneration 12 days later. Plucking 200 hairs in a 12 mm diameter area (100 mm² area; low density plucking) fails to induce follicle regeneration even 30 days later. (C) Plucking induces regeneration of all follicles (the 200 plucked and 600 unplucked) within the plucked area (red circle, 5 mm in diameter). Unplucked follicles (400 HF's in total) outside the plucked area boundary then regenerate due to hair wave propagation (blue circle). (D) High power view showing unplucked follicle regeneration: the old gray club hair (yellow) is

pushed out by the regenerating black anagen hair (red). **(E)** In this schematic drawing, grey dots represent telogen HFs. Black lines encircle exemplary plucked regions. Plucked follicles (purple dots). Regenerating plucked HFs (green dots). Regenerating unplucked HFs (tan dots). **(F)** Plot showing the hair regeneration response versus the size of the plucked field. For all different field sizes, 200 hairs are plucked evenly dispersed throughout the field. A regenerative response is observed when 200 hairs are plucked at a density above a threshold (10 hairs/mm^2), which corresponds to plucking 200 hairs from a 5 mm diameter circular surface area (red line). Three responses represented by different colors (grey, tan, green), are observed (please see text for explanation). The quorum sensing zone is highlighted in orange. See also Figure S1, S2.

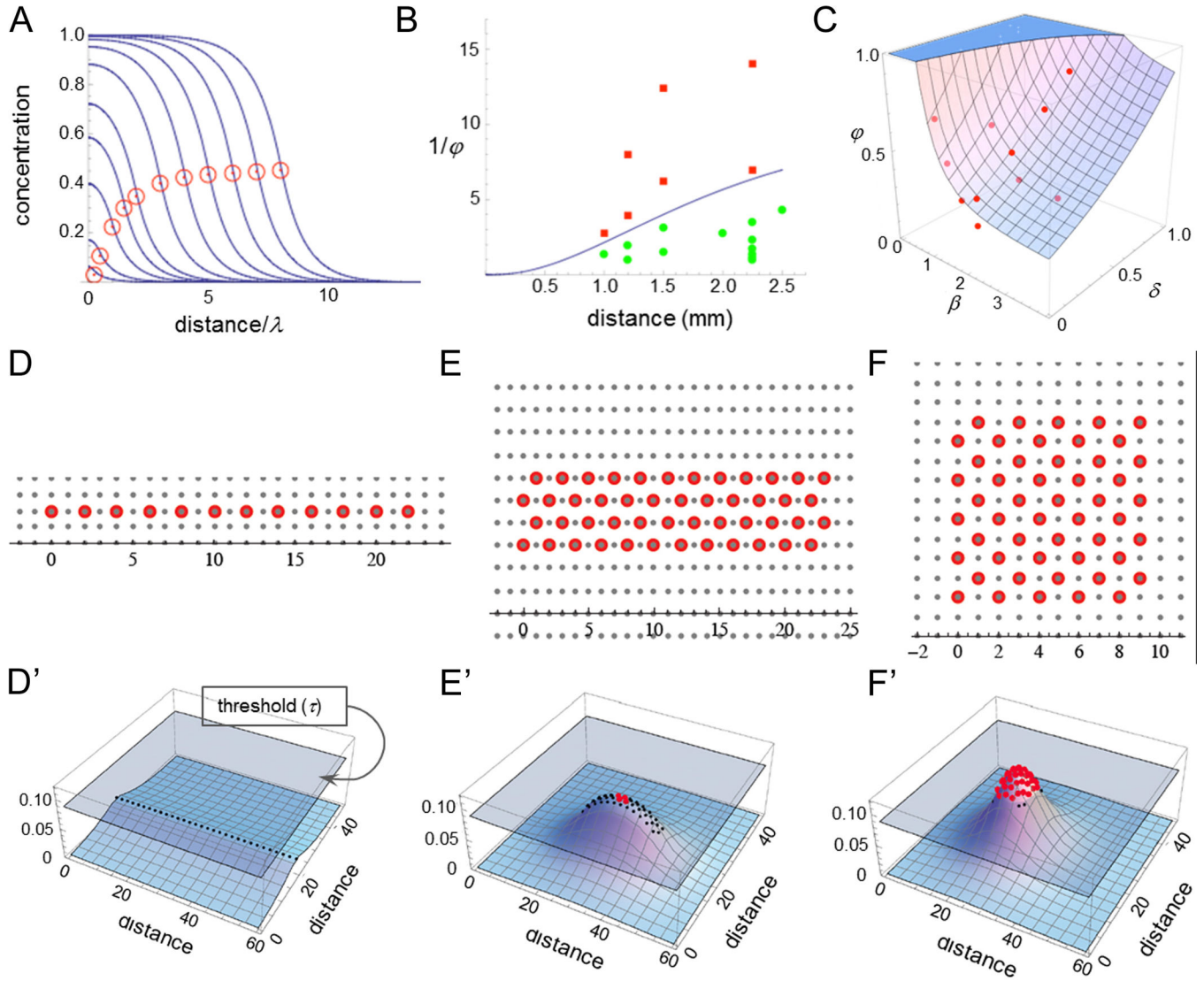


Fig. 2. Mathematical modeling identifies the decay length of a putative quorum signal
(A) Calculated steady state concentrations for a diffusible substance produced within injury fields in proportion to the numbers of plucked HF. Each curve represents a different sized circular injury field, with the red circle placed at the value on the abscissa corresponding to the injury field radius, in units of the diffusing substance decay length. Specifically, the 11 curves represent increasing field sizes of 0.25, 0.5, 1, 1.5, 2, 3, 4, 5, 6, 7 and 8 decay lengths. As plucked regions grow larger, the value at the boundary asymptotes to one half the value at the center. λ is a decay length. Please see Results and supplements for more explanation.
(B) Data from a variety of regeneration experiments involving circular wound fields are plotted as a function of the inverse of the plucked fraction (ϕ) and the radius of the wound field. The curve drawn between the points corresponding to cases of successful (green) and unsuccessful (red) regeneration was obtained from the equations that produced the curves in panel A, by fitting two parameters, the decay length and the threshold concentration for regeneration. The range of possible values consistent with the data was manually explored to yield a range of decay length estimates.
(C) The same model was used as in panel B, but the

data that were fit consisted of the distances, δ , just beyond the edges of injury fields at which initial regeneration was seen. (β , radius of the injury field; ϕ , the plucked fraction). The plotted surface represents a least-squares best fit to the data. (**D–F, D’–F’**) Effects of injury field shape. 50 hairs were plucked evenly, at a density of every other hair, either in a straight line (**D, D’**), a narrow rectangle (6:1 aspect ratio; **E, E’**) or a square (**F, F’**). In **D’–F’**, a discrete form of the equation used in panels A–C, in which each HF is modeled as a discrete source, was used to plot the steady-state spatial distributions of a distressor released by plucked follicles (distances are plotted in units of the inter-follicular distance, about 0.15 mm). Wherever plotted surfaces extend above a regeneration concentration threshold (grey plane), red dots mark the location of each HF indicating successful regeneration. The requirement that these curves be consistent with the observed regeneration patterns in all three cases was sufficient to provide yet a third estimate of the distressor decay length. See also supplement on mathematical model.

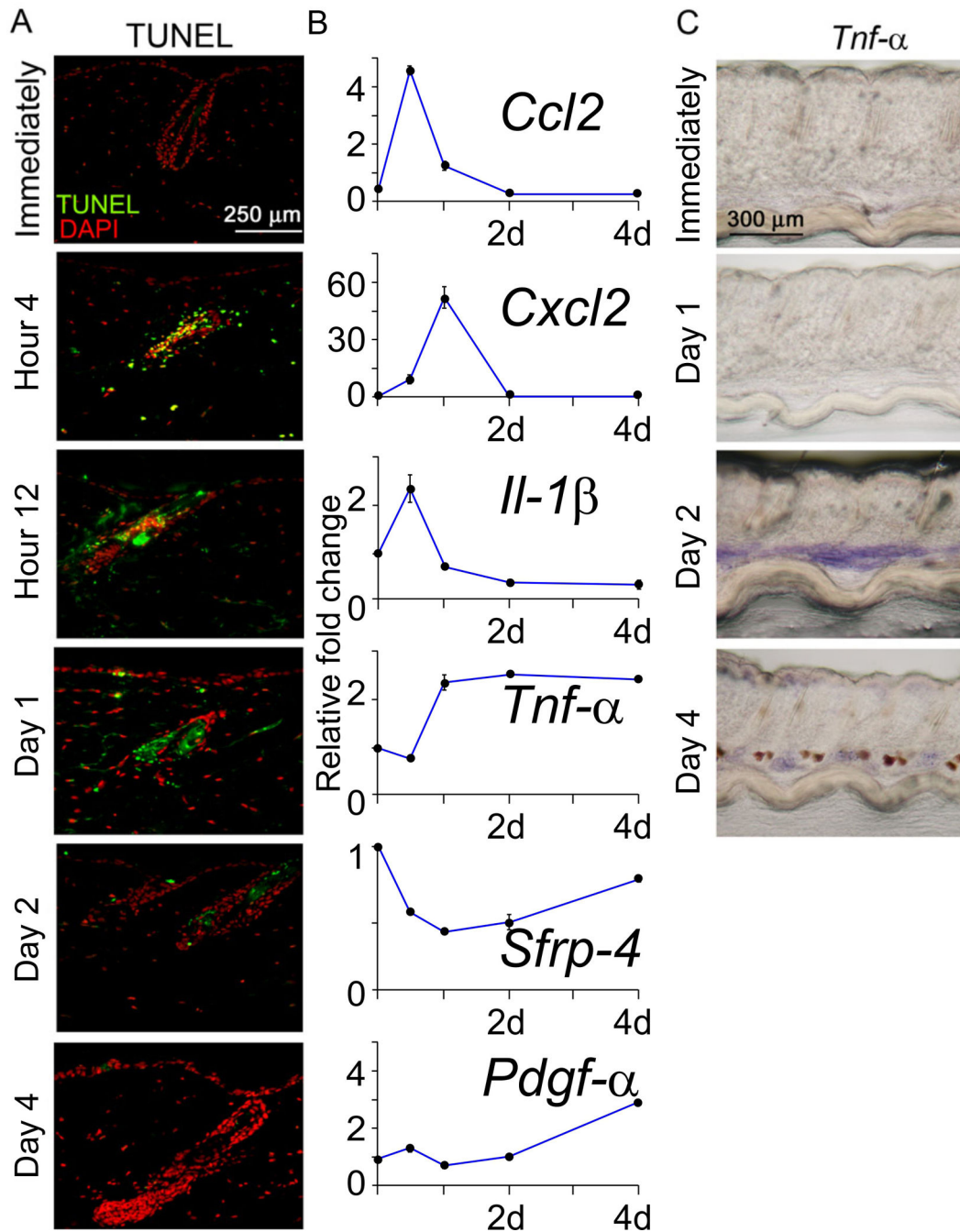


Figure 3. Identification of macro-environmental modulators following hair plucking (A) TUNEL assay to measure apoptosis. (B) Real time PCR from extra-follicular macro-environmental tissues revealed the kinetics of gene expression induced by plucking (Normalized to GAPDH with 40 cycles, data are represented as mean \pm S.D., n=3). (C) Whole mount in situ hybridization showed that *Tnf- α* is markedly up-regulated in the inter-follicular area beginning 2 days after wax stripping. See also Figure S3, S4.

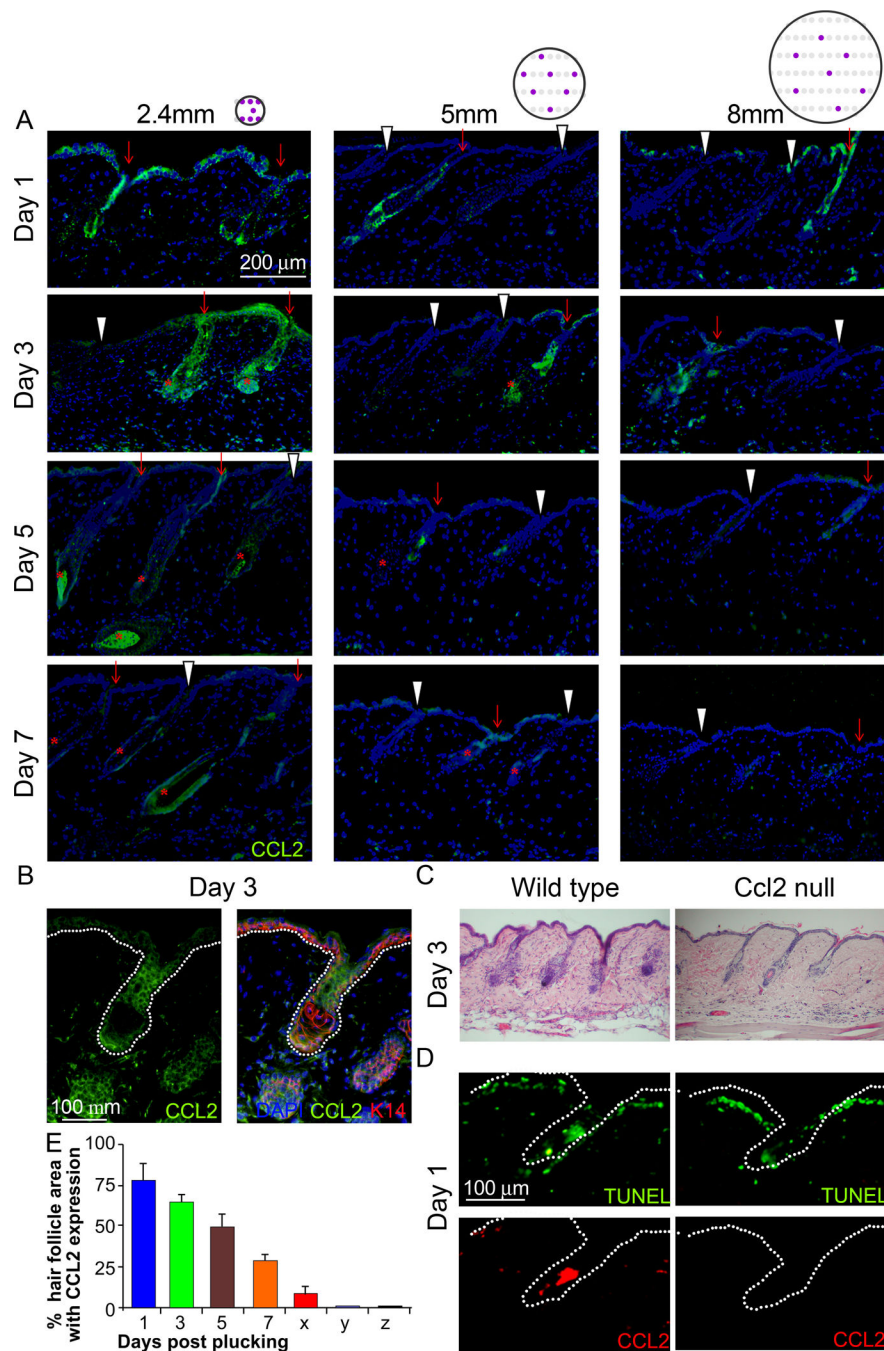


Figure 4. CCL2 is involved in plucking induced hair regeneration

(A) HF keratinocytes showed higher CCL2 expression (green) in plucked follicles (red arrow) than in unplucked follicles (white arrowhead). The circle with purple dots indicates the topology of plucked follicles (please also see Fig. 1E). Peak expression occurs 1–3 days after plucking, and no marked difference between the 2.4, 5 and 8mm groups were noted. (*: Regenerating HF) (B) Double immunostaining for K14 and CCL2 of samples 3 days after plucking showed that HF keratinocytes in plucked follicles are the main source of CCL2. (C) Hair re-growth is retarded when hairs were plucked from CCL2 null mice. (D) CCL2

null mice showed similar apoptotic HF cells following plucking as wild type mice, but couldn't induce CCL2 in apoptotic HF cells. (E) Graph showing the percentage of HF area expressing CCL2 at 1, 3, 5 and 7 days post plucking as well as unplucked HFs within (x) and outside (y) of the plucked field. CCL2 null mice do not express CCL2 (z). (n=3). (Data are represented as mean \pm S.D.). See also Figure S5.

Author Manuscript

Author Manuscript

Author Manuscript

Author Manuscript

density decreases with increasing distance from the plucked follicles. See Fig. S7A for the unit area we quantified for each data point. The number of F4/80+ cells is rapidly elevated at day 1 post-plucking, reaching a maximum at day 3 and then diminishing at 5 and 7 days after plucking. **(F)** *LysM-Cre;R26R* reporter mice show that the myeloid lineage-derived cells mostly are induced in the dermis around plucked HFs. **(G)** When 200 hairs were plucked from myeloid cell deficient mice from 5 mm region, hairs cannot be induced. **(H)** Tnf- α (+) cells was not induced in CCL2 null mice. **(I)** Tnf- α serum levels are similar between wild type and CCL2 null mice. (Data are represented as mean \pm S.D.). See also Figure S6–7.

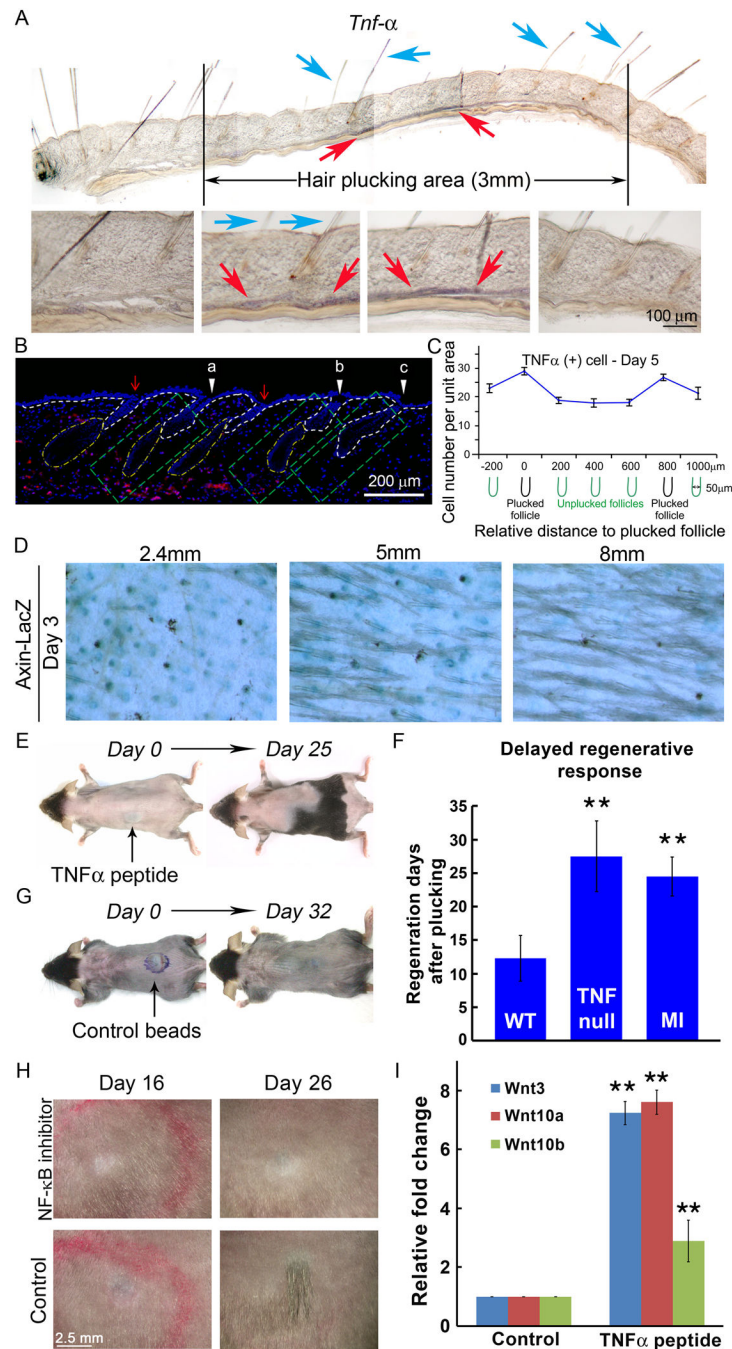


Figure 6. Hair regeneration is proportional to the local concentration of Tnf- α
(A) Whole mount in situ hybridization shows Tnf- α (brown color in the dermis, red arrows) was induced under plucked and unplucked hairs (blue arrows) toward the center of the 3mm plucked zone 5 days after plucking. **(B)** Semi-quantitative assessment of the Tnf- α concentration using the 5mm group at day 5. Its expression level was quantified in 3 different skin regions (green boxes) that differ in their proximity to plucked follicles. “a” is closest to the plucked follicles and shows the highest Tnf- α levels. “b” is away from the plucked follicles and shows lower Tnf- α levels. “c” is furthest away and shows the least

Tnf- α . **(C)** Quantitative assessment of the Tnf- α positive cells around plucked follicles and inter-plucked follicle dermis. See Fig. S7B for complete series. The pattern is similar to that of F4/80 macrophage distribution. (n=3) **(D)** Density-dependent plucking on *Axin-LacZ* mice show that the canonical Wnt/ β -catenin signaling pathway was activated 3 days after plucking and the number of LacZ (+) HF's was proportional to the plucking density. **(E)** Subcutaneous injection of Tnf- α related peptide coated beads during refractory telogen can induce anagen re-entry and then propagate to the surrounding HF's. **(F)** Tnf- α null mice exhibit a 15-day delay in anagen re-entry following plucking of 200 hairs during refractory telogen phase. Intra-peritoneal macrophage inhibitor (MI) injection can also delay plucking induced hair regeneration by 12 days. **(G)** Albumin coated beads injection showed no anagen re-entry even after 32 days. **(H)** Subcutaneous NF- κ B inhibitor injection can delay plucking-induced hair regeneration by 10 days. **(I)** Wnt3, Wnt10a and Wnt10b were activated in keratinocytes by TNF related peptides. (Data are represented as mean \pm S.D., ** p < 0.001). See also S6-7.

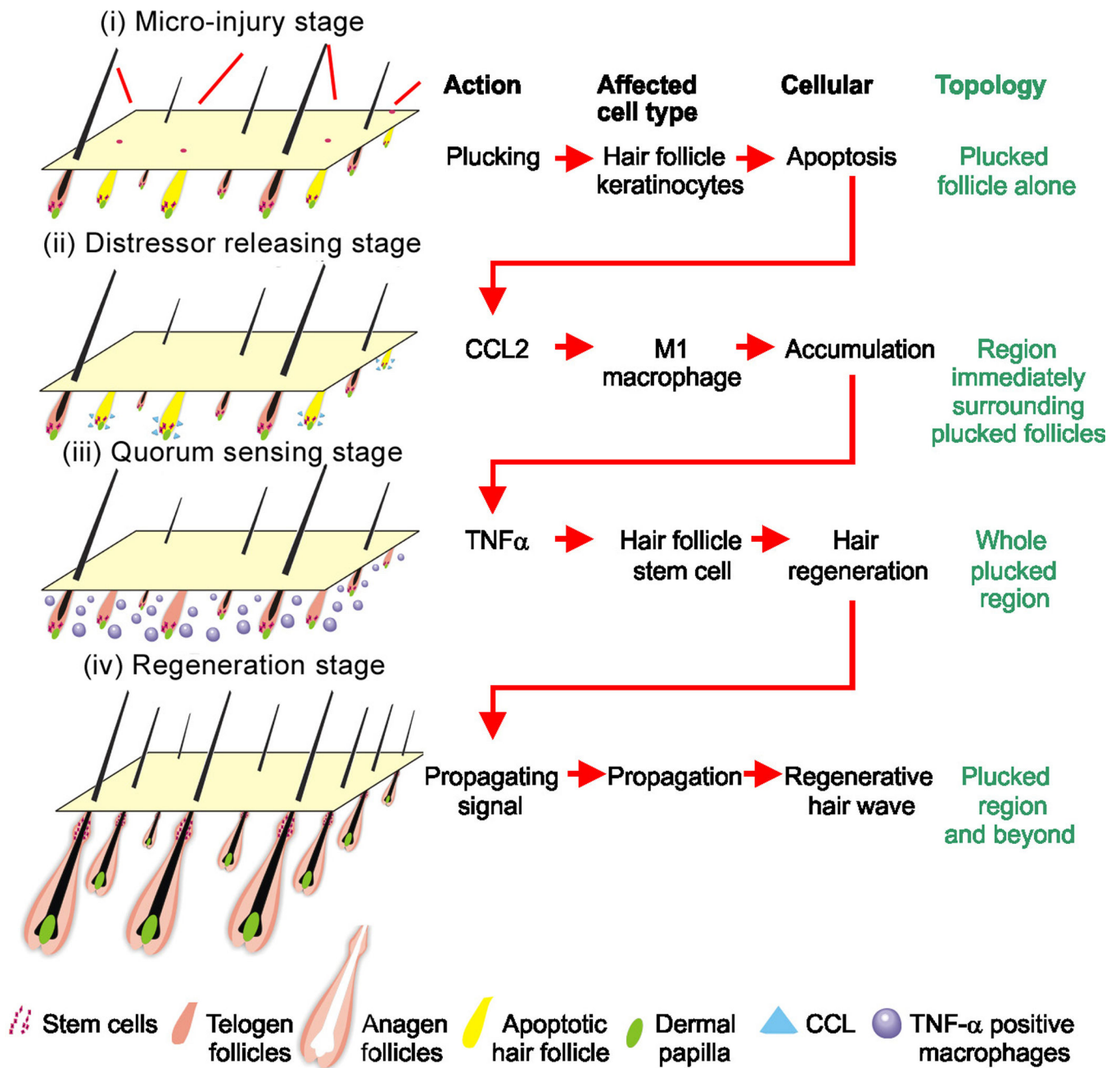


Fig. 7. Molecular basis of quorum sensing behavior during the activation of hair stem cells in the follicle population

Schematic illustration of the process. Stage i: Minor-injury \rightarrow hair keratinocyte apoptosis \rightarrow CCL2 production. Stage ii: CCL2 secretion \rightarrow macrophage accumulation, Stage iii: Macrophage and Tnf- α permeate the whole region. Stage iv: Tnf- α activates hair regeneration in the whole region. Hair regeneration further spreads due to propagation of regenerative hair waves. Please see text for more detail of the model.